Iberian Strings
Bilbao 31 January 2012

Holographic Bottom-up models for YM and QCD.

Elias Kiritsis

University of Crete APC, Paris

Bibliography

Based on earlier work by

Umut Gursoy, Liuba Mazzanti, George Michalogiorgakis, Fransesco Nitti, arXiv:1006.5461 [hep-th]

recent work with:

Matti Jarvinnen (Crete) arXiv:1112.1261 [hep-ph]

and ongoing work with:

T. Alho (Helsinki), D. Arean (SISSA) I. Iatrakis (Crete), M. Jarvinnen (Crete), K. Kajantie (Helsinki), K. Tuominnen (Helsinki).

Introduction

- Holography is providing a new window to strong coupling physics.

- It has been instrumental in understanding non-perturbative phenomena that pertain to QCD.

- Although a fully controlable YM dual is lacking, bottom-up models inspired and constrained by string theory can describe reasonably well the YM physics.

• For several phenomena in QCD the presence of quarks is important ($SU(N_c)$ theory with N_f quarks).

• Sometimes the relevant physics can be studied in the "Quenched Approximation": quarks are probes in the glue dynamics.

• For others however, one should include propagating quarks inducing quantum corrections in order to see them. In this second class we can mention:

♠ The conformal window: the theory flows to an IR CFT for $x \equiv \frac{N_f}{N_c} \geq x_c$ if quarks are massless. Chiral symmetry is expected to remain unbroken in this phase. The conformal window ends at the Banks-Zaks point, $x = \frac{11}{2}$.

♠ The phase transition at $x = x_c$ that is expected from some approximate arguments to be in the BKT class. This type of transition where for $x < x_c$ there is a condensate is known as a conformal transition.

Miransky, Kaplan+Stephanov+Son

♠ The region just below x_c where the theory is expected to exhibit walking behavior. This type of behavior is useful for technicolor models.

♠ The QCD thermodynamics as a function of x.

♠ The phase diagram as a function of baryon density. Here we expect a color superconducting phase, as well as a color-flavor locking phase.

Alford+Rajagopal+Wilczek

• All of the phenomena above except the Banks-Zaks region are at strong coupling and therefore hard to analyze.

• Several (uncontrolable) techniques were applies so far for their study: Truncated Schwinger-Dyson equations, lattice calculations, guesswork on β functions, etc. It is with such techniques that some of the expectations above were found.

The holographic models: glue

For YM, ihQCD is a well-tested holographic, string-inspired bottom-up model with action

Gursoy+Kiritsis+Nitti, Gubser+Nelore

$$\mathcal{S}_{\rm g} = M^3 N_c^2 \int d^5x \sqrt{g} \left[R - \frac{4}{3}(\partial\phi)^2 + V_g(\phi) \right]$$

- $g_{\mu\nu}$ is dual to $T_{\mu\nu}$

- ϕ is dual to $tr[F^2]$.

We expect that these two operators capture the important part of the dynamics of the YM vacuum.

- The potential $V_g \leftrightarrow$ QCD β-function

- $A \to \log \mu$ energy scale.

- $e^{\phi} \to \lambda$ 't Hooft coupling

In the UV $\lambda \to 0$ and

$$V_g = V_0 + V_1\lambda + V_2\lambda^2 + \mathcal{O}(\lambda^3)$$

In the IR $\lambda \to \infty$ and

$$V_g \sim \lambda^{\frac{4}{3}}\sqrt{\log\lambda} + \cdots$$

• This was chosen after analysing all possible asymptotics and characterising their behavior.

The IR asymptotics is uniquely fixed by asking for confinement, discrete spectra and asymptotically linear glueball trajectories. *Gursoy+Kiritsis+Nitti*

The vacuum saddle point is given by a Poincaré-invariant metric, and radially depended dilaton.

$$ds^2 = e^{2A}(dr^2 + \eta_{\mu\nu}dx^\mu dx^\nu)$$

• With an appropriate tuning of two parameters in V_g the model describes well both $T = 0$ properties (spectra) as well as thermodynamics.

YM Entropy

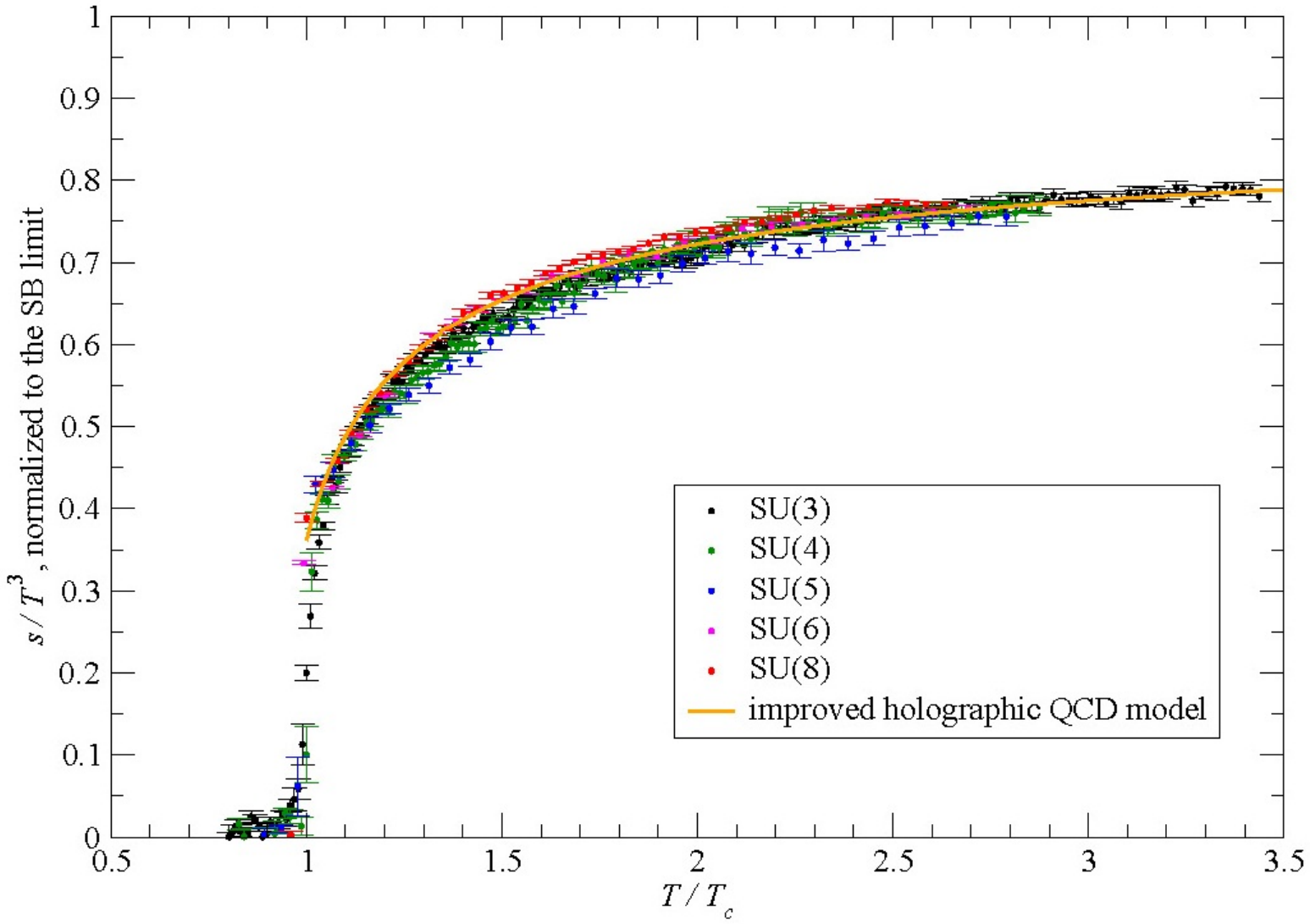

Figure 4: (Color online) Same as in fig. 1, but for the s/T^3 ratio, normalized to the SB limit.

From M. Panero, arXiv:0907.3719

Equation of state

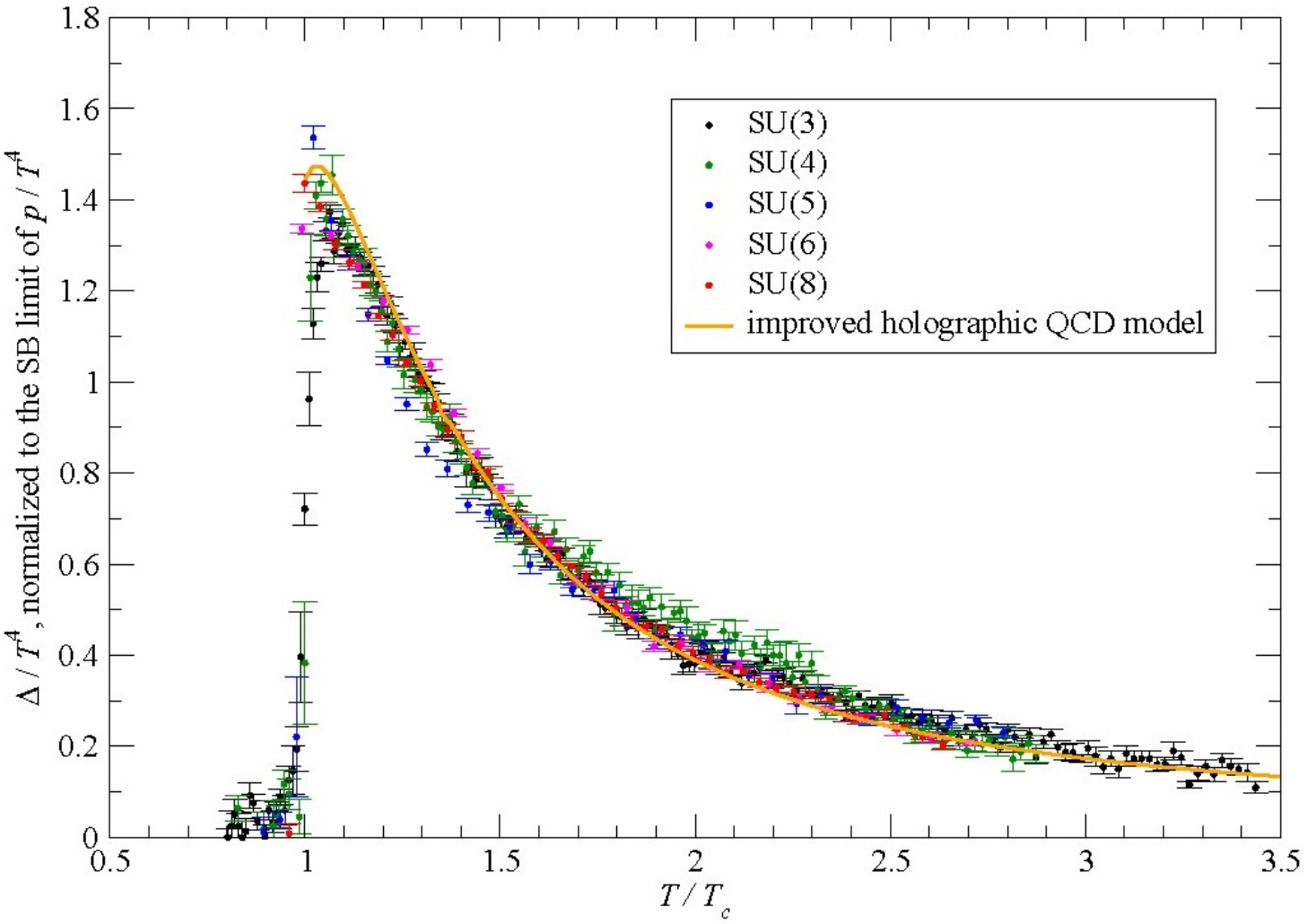

Figure 2: (Color online) Same as in fig. 1, but for the Δ/T^4 ratio, normalized to the SB limit of p/T^4.

From M. Panero, arXiv:0907.3719

The sound speed

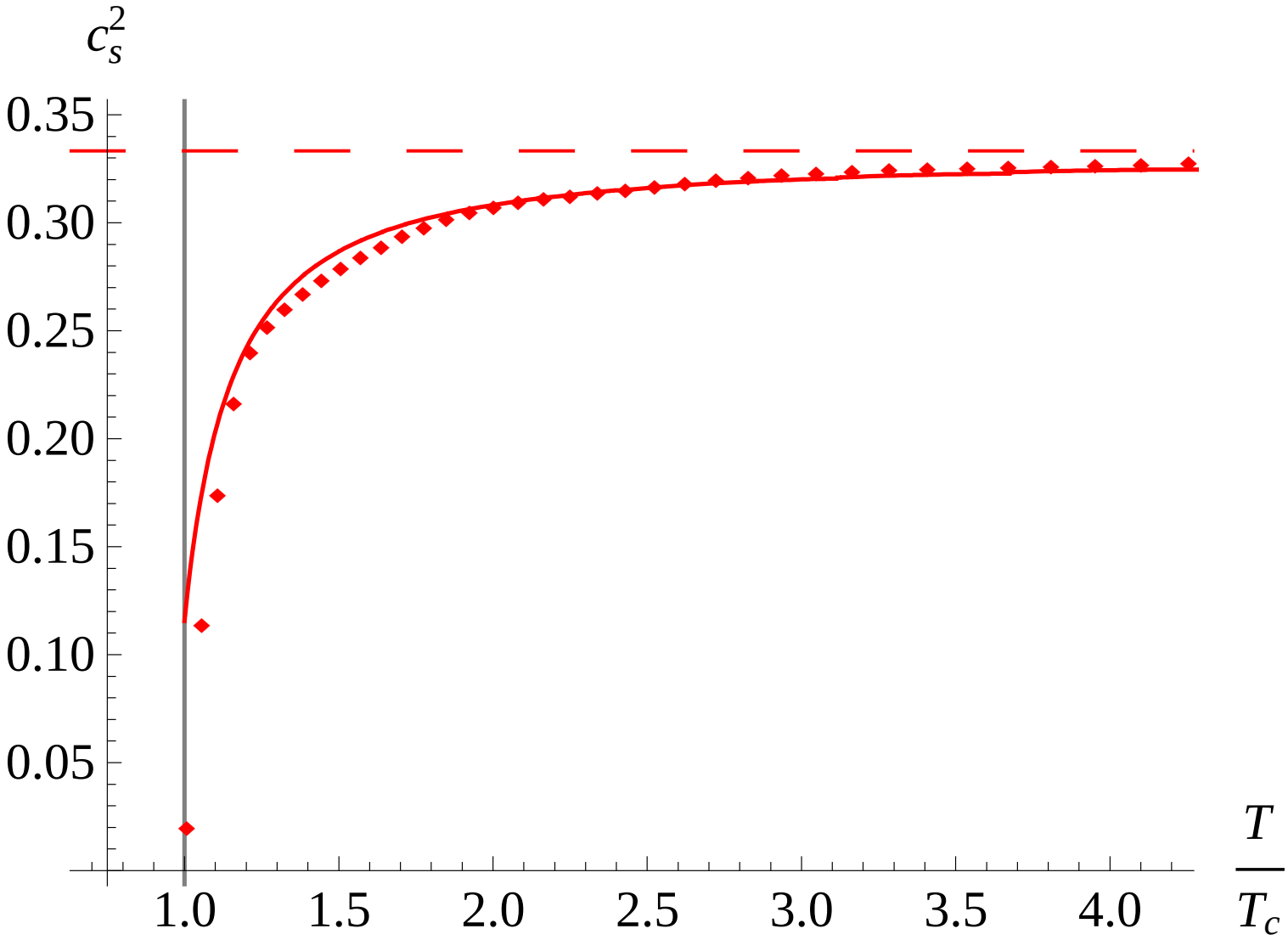

The holographic models: flavor

- Fundamental quarks $\rightarrow$ probe $D4$-$\bar{D}4$ branes in 5-dimensions.

- We have the gauge fields from $D4-D4$ strings A_L^μ and $\bar{D}4-\bar{D}4$ strings A_R^μ dual to J_L^μ and J_R^μ and a tachyon T_{ij} from the $D4-\bar{D}4$ strings dual to the mass operator $\bar{\psi}_L^i \psi_R^j$.

- For the vacuum structure only the tachyon is relevant.

- An action for the tachyon motivated by the Sen action has been advocated as the proper dynamics of the chiral, condensate giving in general all the expected features of χSB.

Casero+Kiritsis+Paredes

$$\mathcal{S}_{\text{TDBI}} = -N_f N_c M^3 \int d^5x \; V_f(T) \; e^{-\phi} \sqrt{-\det(g_{ab} + \partial_a T \partial_b T)}$$

- It has been tested in a 6d asymptotically-AdS confining background (with constant dilaton) due to Kuperstein+Sonneschein.

Iatrakis+Kiritsis+Paredes

It was shown to have the following properties:

- Confining asymptotics of the geometry trigger chiral symmetry breaking.

- A Gell-Mann-Oakes-Renner relation is generically satisfied.

- The Sen DBI tachyon action induces linear Regge trajectories for mesons.

- The Wess-Zumino (WZ) terms of the tachyon action, computed in string theory, produce the appropriate flavor anomalies, include the axial $U(1)$ anomaly and η'-mixing, and implement a holographic version of the Coleman-Witten theorem.

- The dynamics determines the chiral condensate uniquely a s function of the bare quark mass.

- The mass of the ρ-meson grows with increasing quark mass.

- By adjusting the same parameters as in QCD ($\Lambda_{\rm QCD}$, m_{ud}) a good fit can be obtained of the light meson masses.

The Veneziano limit

- The 't Hooft limit

$$N_c \to \infty, \qquad l = g^2_{\rm YM} N_c \to \text{fixed}$$

always samples the quenched approximation as N_f is kept fixed as $N_c \to \infty$.

- The proper limit in order to study the previous phenomena in the large N_c approximation is the limit introduced by Veneziano

$$N_c \to \infty \quad , \quad N_f \to \infty \quad , \quad \frac{N_f}{N_c} = x \to \text{fixed} \quad , \quad \lambda = g^2_{\rm YM} N_c \to \text{fixed}$$

- In terms of the dual string theory, the boundaries of diagrams are not suppressed anymore: surfaces with an arbitrary number of boundaries contribute at the same order (for the flavor singlet sector).

The Banks-Zaks region

- The QCD β function in the V-limit is

$$\dot{\lambda} = \beta(\lambda) = -b_0\lambda^2 + b_1\lambda^3 + \mathcal{O}(\lambda^4) \ , \ b_0 = \frac{2}{3}\frac{(11-2x)}{(4\pi)^2} \ , \ \frac{b_1}{b_0^2} = -\frac{3}{2}\frac{(34-13x)}{(11-2x)^2}$$

- The Banks-Zaks region is $x = 11/2 - \epsilon$ with $\epsilon \ll 1$ and positive. We obtain a fixed point of the β-function at $\lambda_* \simeq \frac{(8\pi)^2}{75}\epsilon + \mathcal{O}(\epsilon^2)$ which is trustable in perturbation theory, as λ_* can be made arbitrarily small.
- The mass operator, $\bar{\psi}_L\psi_R$ has now dimension smaller than three, from the perturbative anomalous dimension (in the V-limit)

$$-\frac{d\log m}{d\log\mu} \equiv \gamma = \frac{3}{(4\pi)^2}\lambda + \frac{(203-10x)}{12\,(4\pi)^4}\lambda^2 + \mathcal{O}(\lambda^3, N_c^{-2})$$

- Extrapolating to lower x we expect the phase diagram

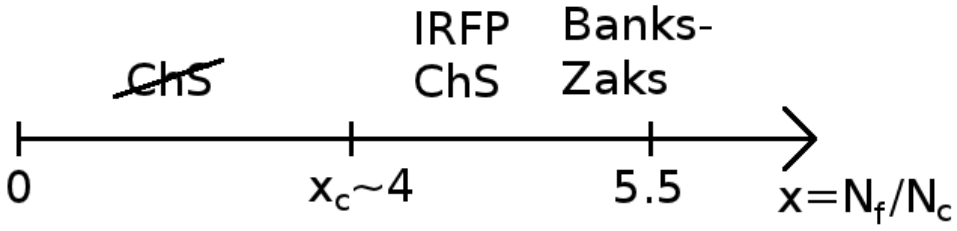

Fusion

The idea is to put together the two ingredients in order to study the chiral dynamics and its backreaction to glue.

$$\mathcal{S} = M^3 N_c^2 \int d^5x \sqrt{g} \left[R - \frac{4}{3} \frac{(\partial\lambda)^2}{\lambda^2} + V_g(\lambda) \right] -$$

$$- N_f N_c M^3 \int d^5x V_f(\lambda, T) \sqrt{-\det(g_{ab} + h(\lambda) \partial_a T \partial_b T)}$$

with $V_f(\lambda, T) = V_0(\lambda) \exp(-a(\lambda) T^2)$

- V-limit: $N_c \to \infty$ with $x = N_f/N_c$ fixed: backreacted system.
- Probe limit $x \to 0 \Rightarrow V_g$ fixed as before.
- We must choose $V_0(\lambda), a(\lambda), h(\lambda)$.

♠ The simplest and most reasonable choices, compatible with glue dynamics do the job!

The effective potential

For solutions $T = T_* = constant$ the relevant non-linear action simplifies

$$\mathcal{S} = M^3 N_c^2 \int d^5x \sqrt{g} \left[R - \frac{4}{3} \frac{(\partial\lambda)^2}{\lambda^2} + V_g(\lambda) - x V_f(\lambda, T) \right]$$

$$V_{\text{eff}}(\lambda) = V_g(\lambda) - x V_f(\lambda, T_*) = V_g(\lambda) - x V_0(\lambda) \exp(-a(\lambda) T_*^2)$$

• Minimizing for T_* we obtain $T_* = 0$ and $T_* = \infty$. The effective potential for λ is

♠ $T_* = 0$, $V_{eff} = V_g(\lambda) - x V_0(\lambda)$

♠ $T_* = \infty$, $V_{eff} = V_g(\lambda)$ with no fixed points.

$$V_{\rm eff}(\lambda) = V_g(\lambda) - xV_0(\lambda)$$

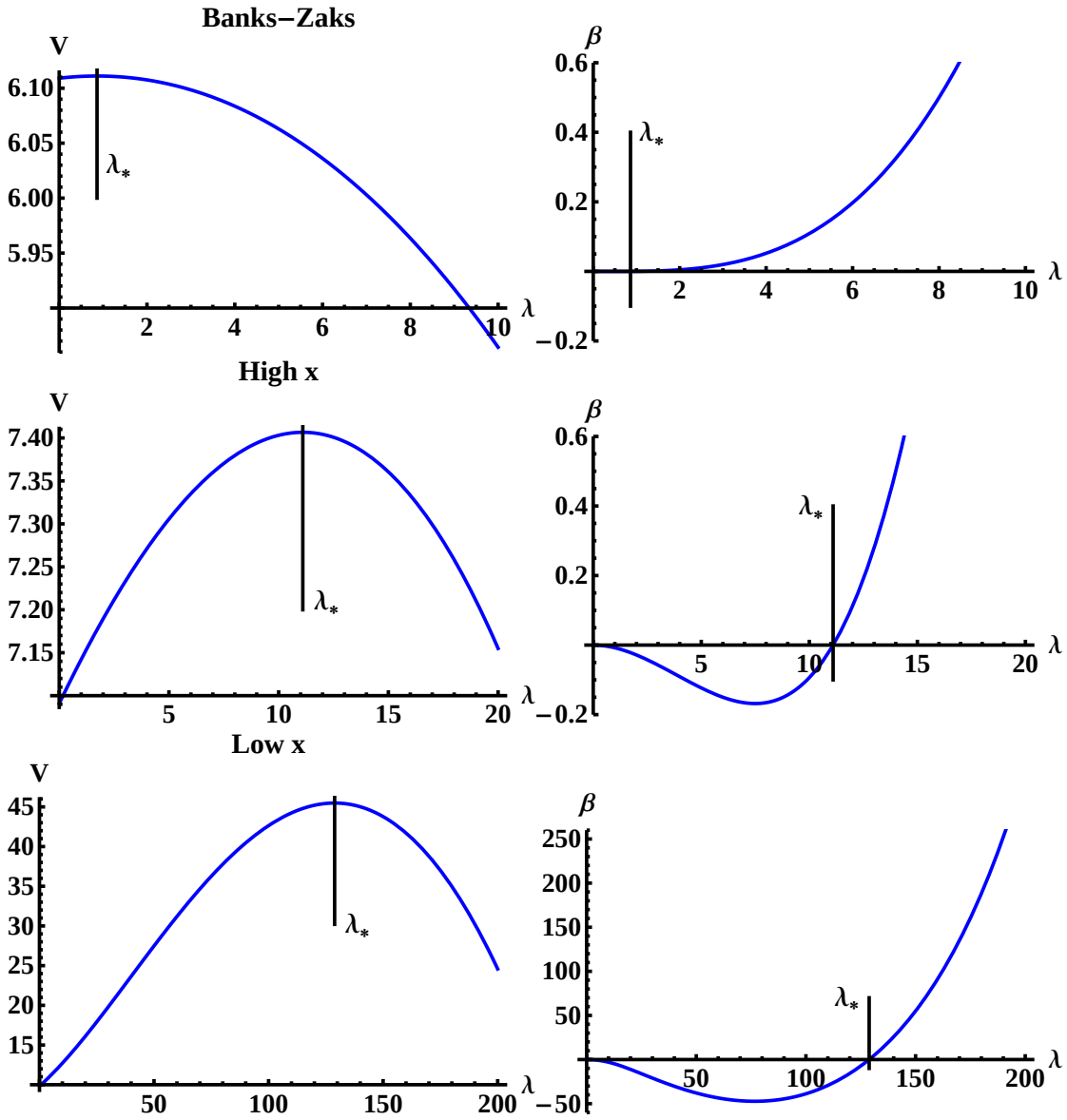

Two possibilities: (a) The maximum exists for all x. (b) The maximum exists for $x > x_*$.

Condensate dimension at the IR fixed point

• By expanding the DBI action we obtain the IR tachyon mass at the IR fixed point $\lambda = \lambda_*$ which gives the chiral condensate dimension:

$$-m_{\rm IR}^2 \ell_{\rm IR}^2 = \Delta_{\rm IR}(4-\Delta_{\rm IR}) = \frac{24a(\lambda_*)}{h(\lambda_*)(V_g(\lambda_*) - xV_0(\lambda_*))}$$

• Must reach the Breitenlohner-Freedman (BF) bound (horizontal line) at some x_c.

• x_c marks the *conformal phase transition*

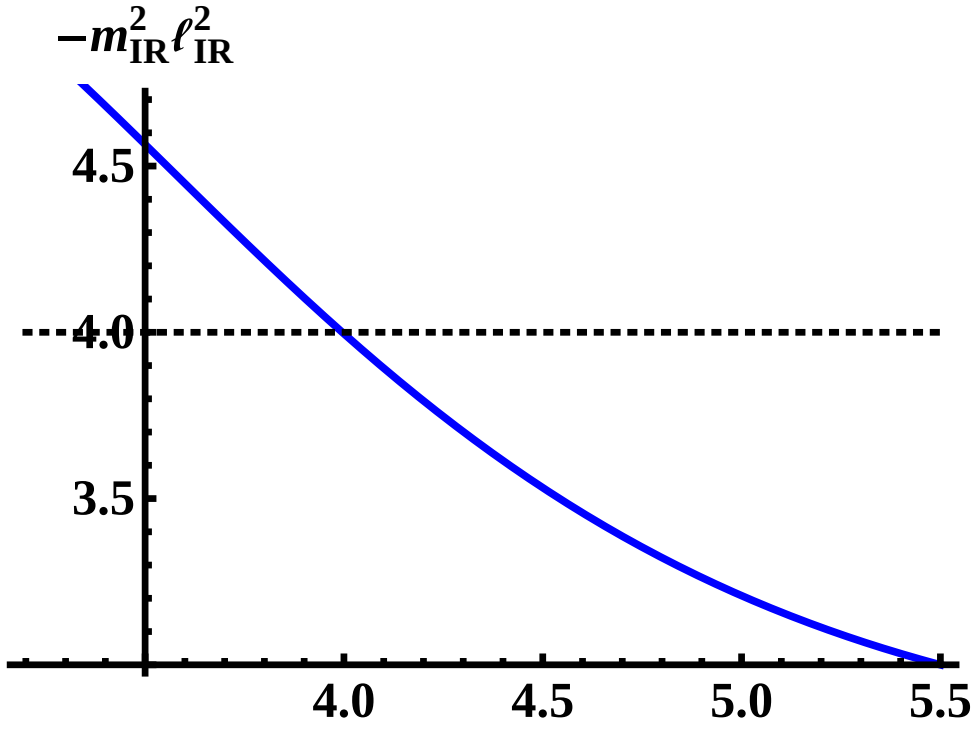

Below the BF bound

- Correlation of the violation of BF bound and the conformal phase transition

- For $\Delta_{\rm IR}(4-\Delta_{\rm IR})<4$

$$T(r)\sim m_q r^{4-\Delta_{\rm IR}}+\sigma r^{\Delta_{\rm IR}}$$

- For $\Delta_{\rm IR}(4-\Delta_{\rm IR})>4$

$$T(r)\sim C r^2 \sin\left[(\mathrm{Im}\Delta_{\rm IR})\log r+\phi\right]$$

Two possibilities:

- $x>x_c$: BF bound satisfied at the fixed point $\Rightarrow$ only trivial massless solution ($T\equiv 0$, ChS intact, fixed point hit)

- $x<x_c$: BF bound violated at the fixed point $\Rightarrow$ a nontrivial massless solution exists, which drives the system away from the fixed point.

Conclusion: *phase transition* at $x=x_c$

Matching to QCD: UV

- As $\lambda \to 0$ we can match:

♠ $V_g(\lambda)$ with (two-loop) Yang-Mills β-function.

♠ $V_g(\lambda) - xV_0(\lambda)$ with QCD β-function.

♠ $a(\lambda)/h(\lambda)$ with anomalous dimension of the quark mass/chiral condensate

- The matching allows to mark the BZ point, that we normalize at $x = \frac{11}{2}$.

- After the matching above we are left with a single undetermined parameter in the UV:

$$V_g \sim V_0 + \mathcal{O}(\lambda) \quad , \quad V_0 \sim W_0 + \mathcal{O}(\lambda)$$

$$V_0 - xW_0 = \frac{12}{\ell_{UV}^2}$$

Matching to QCD: IR

• In the IR, the tachyon has to diverge $\Rightarrow$ the tachyon action $\propto e^{-T^2}$ becomes small

♠ $V_g(\lambda) \simeq \lambda^{\frac{4}{3}}\sqrt{\lambda}$ chosen as for Yang-Mills, so that a "good" IR singularity exists etc.

♠ $V_0(\lambda)$, $a(\lambda)$, and $h(\lambda)$ chosen to produce tachyon divergence: there are several possibilities.

♠ The phase structure is essentially independent of IR choices.

Choice I:

$$V_g(\lambda) = 12 + \frac{44}{9\pi^2}\lambda + \frac{4619}{3888\pi^4}\frac{\lambda^2}{(1+\lambda/(8\pi^2))^{2/3}}\sqrt{1+\log(1+\lambda/(8\pi^2))}$$

$$V_f(\lambda, T) = V_0(\lambda)e^{-a(\lambda)T^2}$$

$$V_0(\lambda) = \frac{12}{11} + \frac{4(33-2x)}{99\pi^2}\lambda + \frac{23473 - 2726x + 92x^2}{42768\pi^4}\lambda^2$$

$$a(\lambda) = \frac{3}{22}(11-x)$$

$$h(\lambda) = \frac{1}{\left(1+\frac{115-16x}{288\pi^2}\lambda\right)^{4/3}}$$

For which in the IR

$$T(r) \sim T_0 \exp\left[\frac{81\ 3^{5/6}(115-16x)^{4/3}(11-x)}{812944\ 2^{1/6}}\frac{r}{R}\right] \quad , \quad r \to \infty$$

R is the IR scale of the solution. T_0 is the control parameter of the UV mass.

Choice II:

$$a(\lambda) = \frac{3}{22}(11-x)\frac{1+\frac{115-16x}{216\pi^2}\lambda+\frac{\lambda^2}{\lambda_0^2}}{(1+\lambda/\lambda_0)^{4/3}}$$

$$h(\lambda) = \frac{1}{(1+\lambda/\lambda_0)^{4/3}}$$

for which in the IR

$$T(r) \sim \frac{27\ 2^{3/4}3^{1/4}}{\sqrt{4619}}\sqrt{\frac{r-r_1}{R}} \quad , \quad r \to \infty$$

R is the IR scale of the solution. r_1 is the control parameter of the UV mass.

Varying the model

"prediction" for x_c

After fixing UV coefficients from QCD, there is still freedom in choosing the leading coefficient of V_0 at $\lambda \to 0$ and the IR asymptotics of the potentials

Thick blue $\to V_I$

Thin red $\to V_{II}$

Resulting variation of the edge of conformal window

$$3.7 \lesssim x_c \lesssim 4.2$$

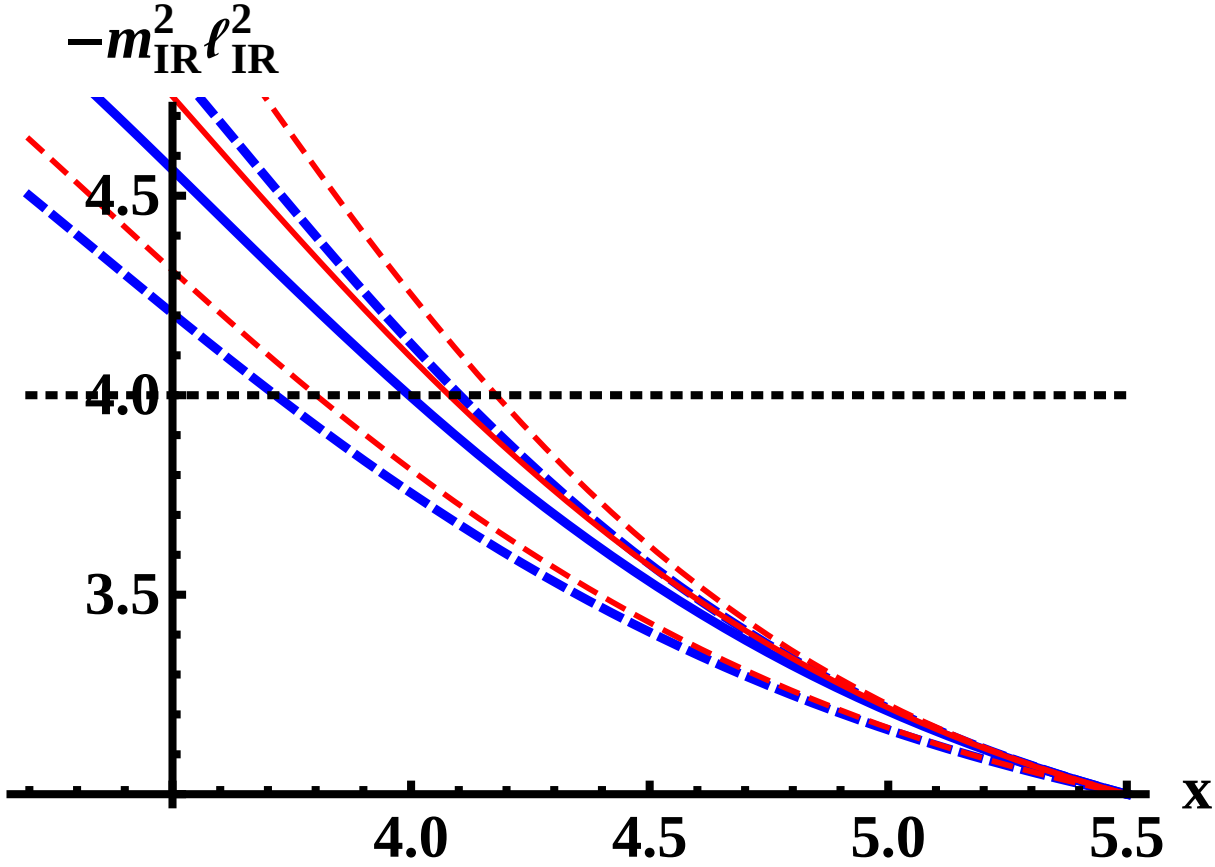

Comparison to previous "guesses"

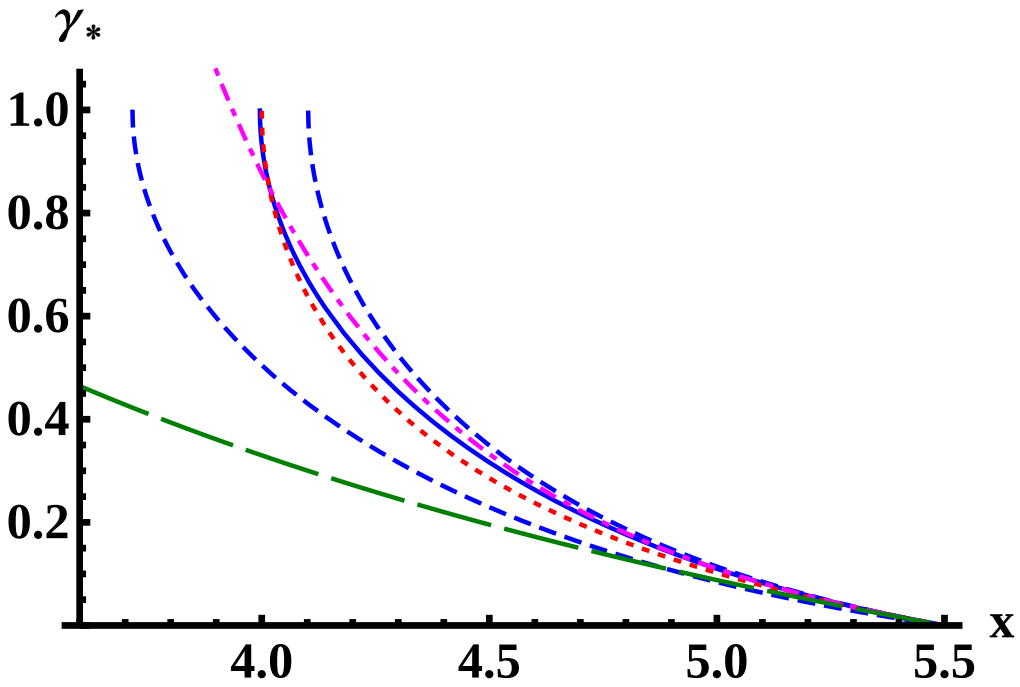

The anomalous dimension of the quark mass at the IR fixed point as a function of x within the conformal window in various approaches.

The solid blue curve is our result for the potential I.

The dashed blue lines show the maximal change as W_0 is varied from 0 (upper curve) to 24/11 (lower curve).

The dotted red curve is the result from a Dyson-Schwinger analysis, the dot-dashed magenta curve is the prediction of two-loop perturbative QCD, and the long-dashed green curve is based on an all-orders β-function.

Holographic β-functions

The second order equations for the system of two scalars plus metric can be written as first order equations for the β-functions

Gursoy+Kiritsis+Nitti

$$\frac{d\lambda}{dA} = \beta(\lambda, T) \quad , \quad \frac{dT}{dA} = \gamma(\lambda, T)$$

The equations of motion boil down to two partial non-linear differential equations for β, γ.

Such equations have also branches as for DBI and non-linear scalar actions the relation of $e^{-A}A'$ with the potentials is a polynomial equation of degree higher than two.

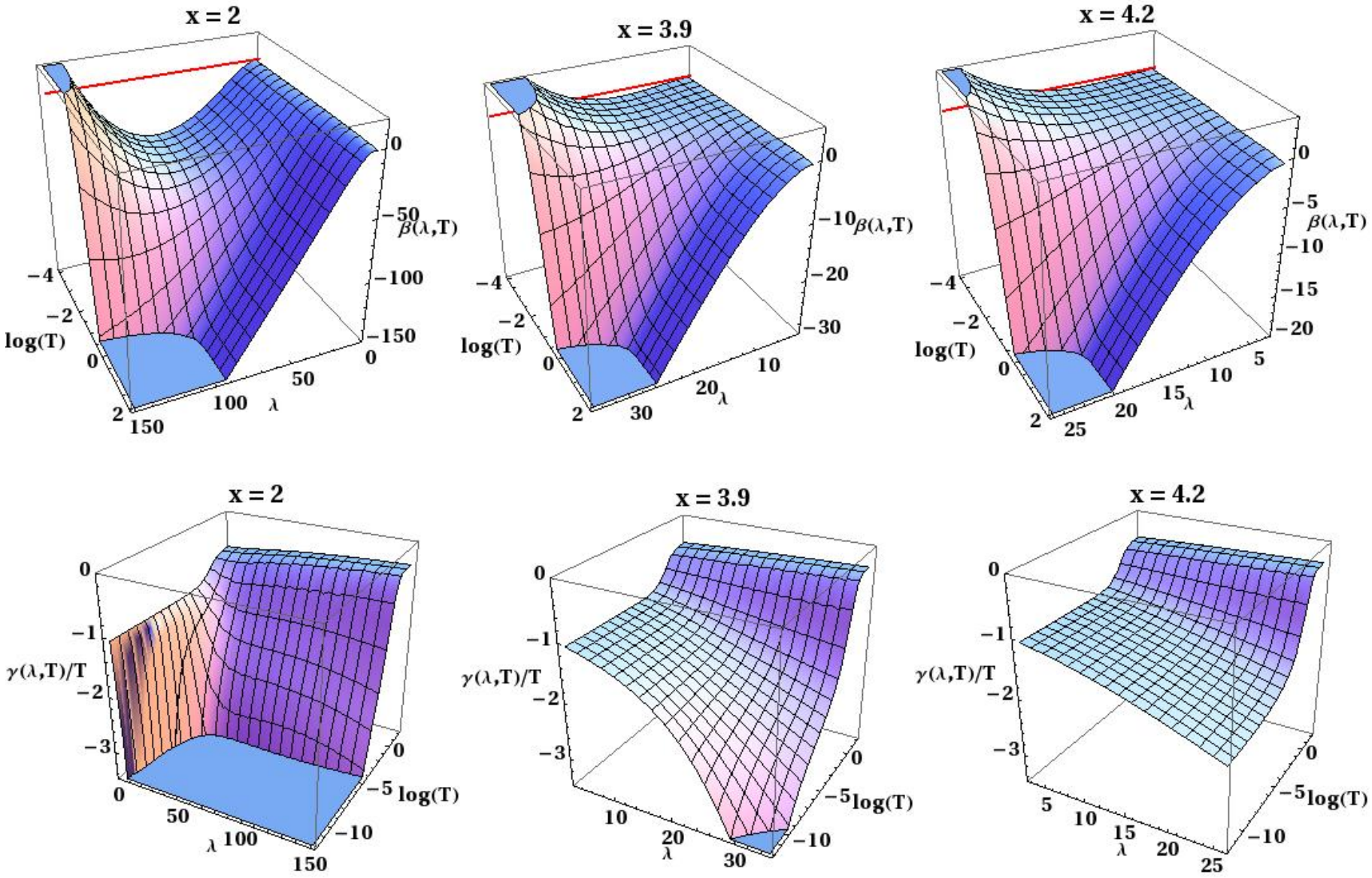

The red lines are added on the top row at $\beta = 0$ in order to show the location of the fixed point.

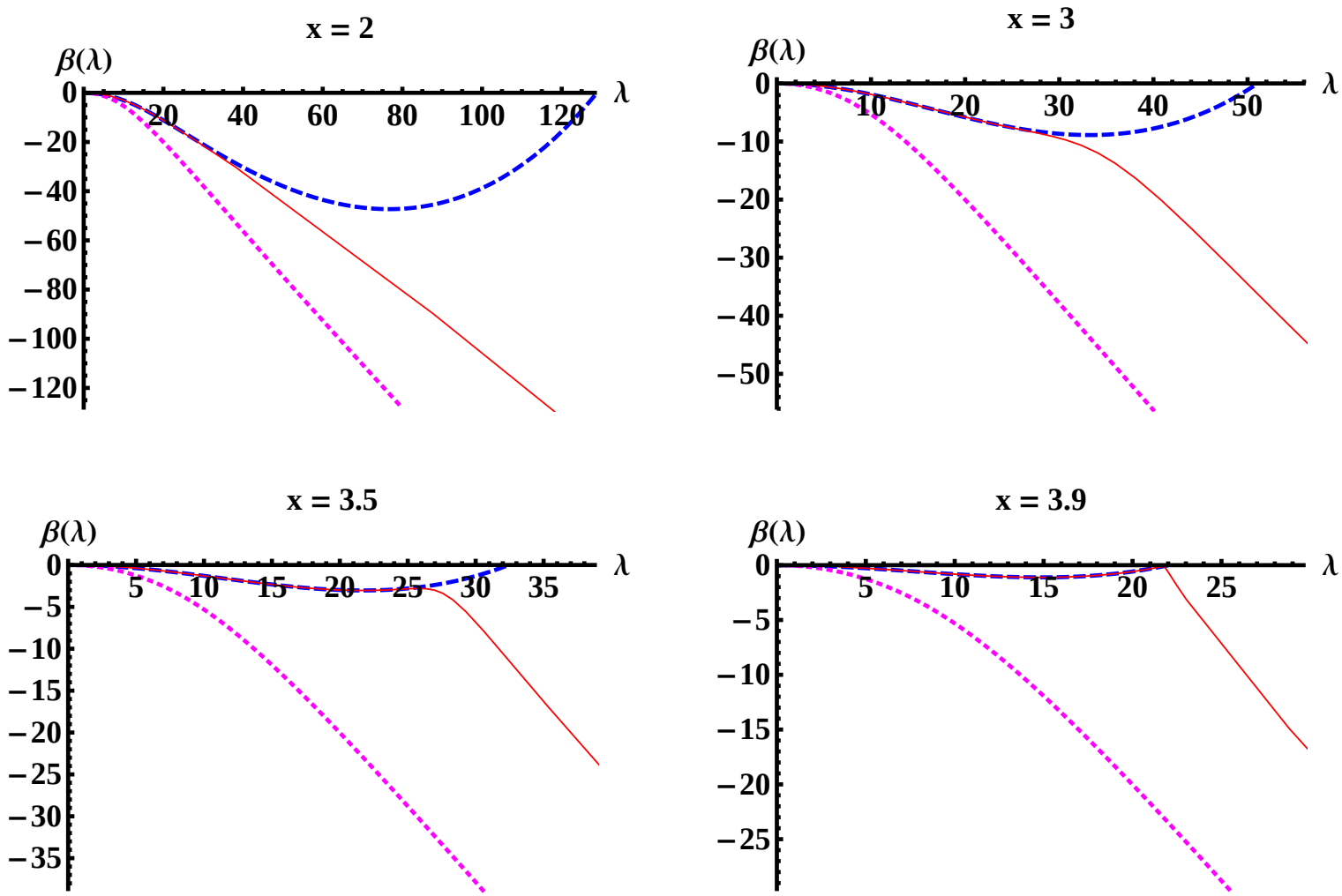

The β-functions for vanishing quark mass for various values of x. The red solid, blue dashed, and magenta dotted curves are the β-functions corresponding to the full numerical solution ($d\lambda/dA$) along the RG flow, the potential $V_{\text{eff}} = V_g - xV_{f0}$, and the potential V_g, respectively.

Parameters

• A theory with a single relevant (or marginally relevant) coupling like YM has no parameters.

• The same applies to QCD with massless quarks.

• QCD with all quarks having mass m has a single (dimensionless) parameter : $\frac{m}{\Lambda_{QCD}}$.

• After various rescalings this single parameter can be mapped to the parameter T_0 that controls the diverging tachyon in the IR.

• There is also x that has become continuous in the large N_c limit.

UV mass vs T_0 and r_1

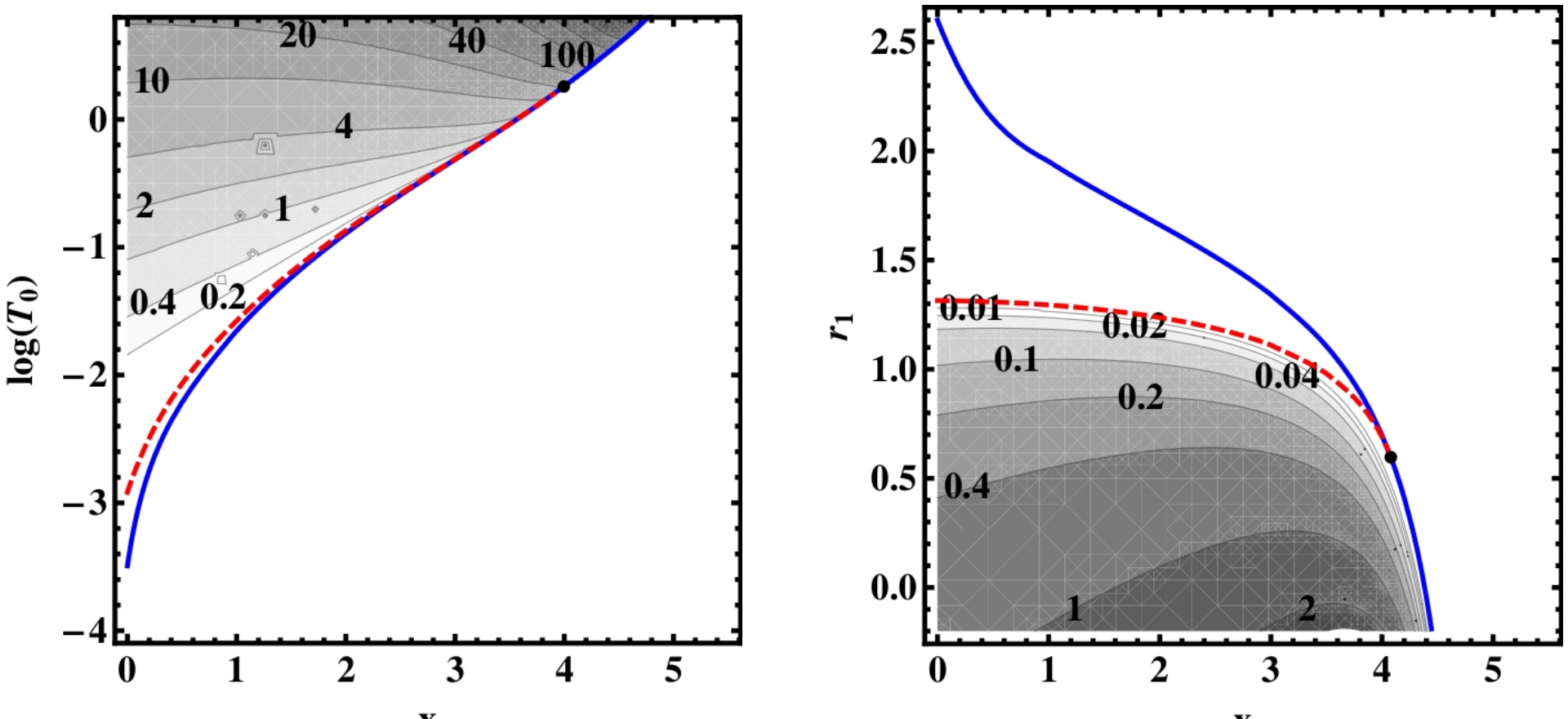

The UV behavior of the background solutions with good IR singularity for the scenario I (left) and parameter T_0 and scenario II (right) and parameter r_1.

The thick blue curve represents a change in the UV behavior, the red dashed curve has zero quark mass, and the contours give the quark mass. The black dot where the zero mass curve terminates lies at the critical value $x = x_c$. For scenario I (II) we have $x_c \simeq 3.9959$ ($x_c \simeq 4.0797$).

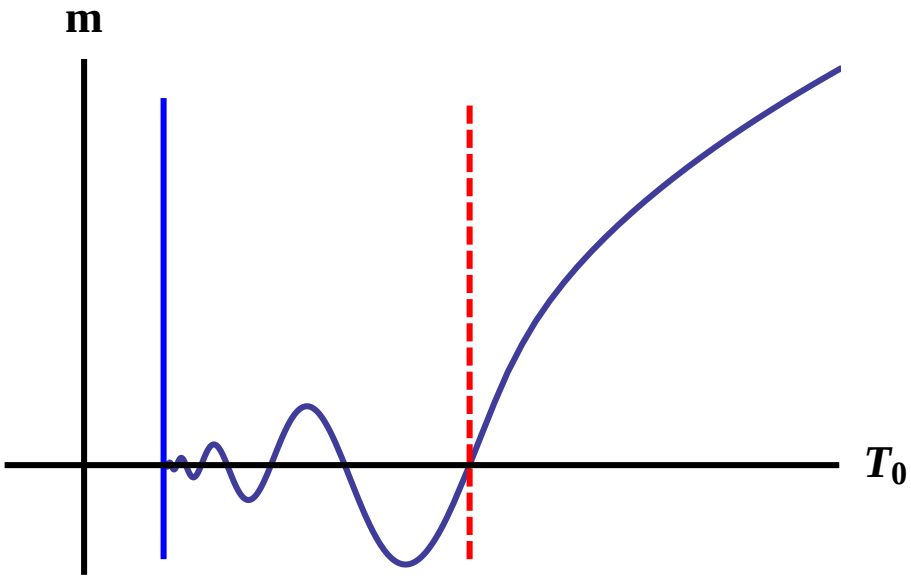

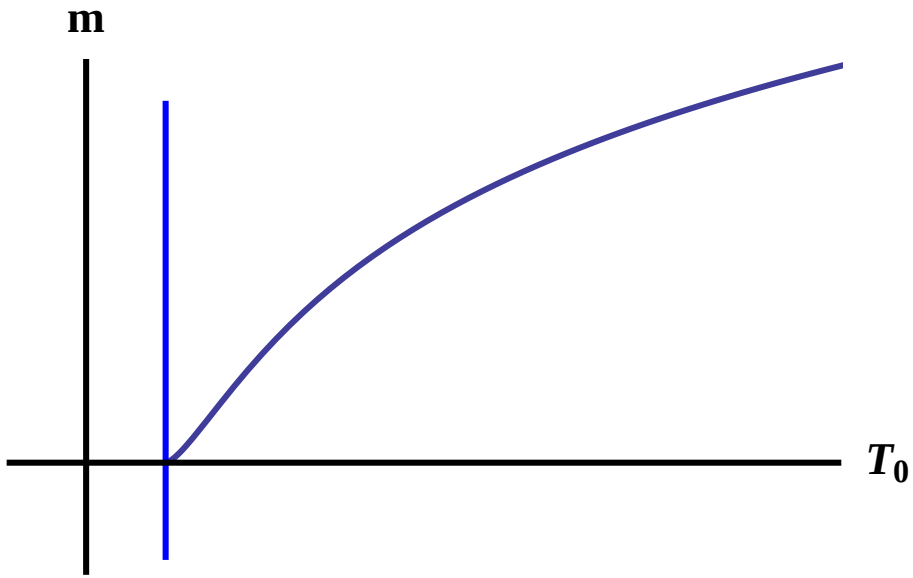

• Left figure: Plot of the UV Mass parameter m, as a function of the IR T_0 scale, for $x < x_c$.

• Right figure: Similar plot for $x \geq x_c$. The vertical solid blue and dashed red lines show where corresponding lines are intersected in previous figures.

• Such plots are sketched from the numerics, analytical expansions and some guesses.

• Near the fixed point value λ_*, the approximate solution of the tachyon is given by $T \sim r^2 \sin[k \log r + \phi]$. The constant k is fixed for fixed x but the normalization and ϕ are determined by the boundary conditions and IR regularity.

• The tachyon starts at the boundary, evolves into the sinusoidal form for a while, and then at the end diverges. Similar behavior seen at

Kutasov+Lin+Parnachev

• Different solutions differ in the region in which they are sinusoidal, and it is this region that controls their number of zeros.

• For the n-th solution, the tachyon changes sign n times times before diverging in the IR.

• At $m = 0$ there is an ∞ number of saddle point solutions (reflecting the Efimov minima)

• They may appear even in the absence of a IR fixed point

The free energy

The free energy difference between the ChS and ChSB $m_q = 0$ solutions

Chiral symmetry breaking solution favored whenever it exists ($x < x_c$)

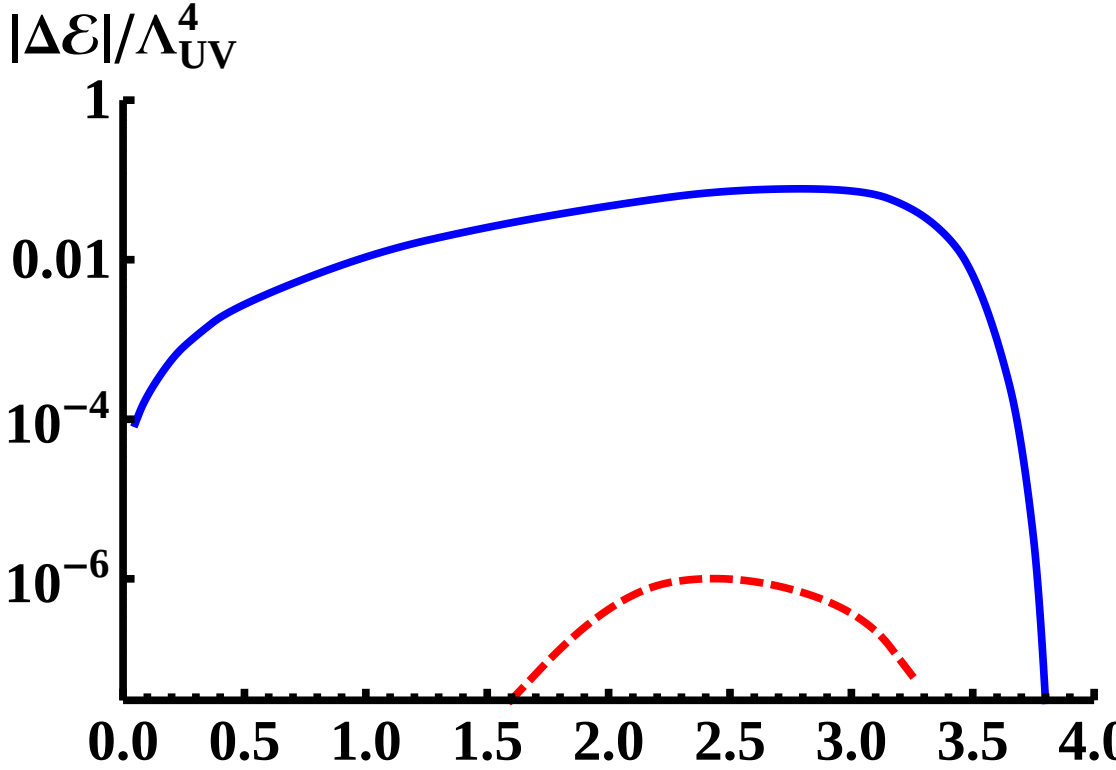

- The Efimov minima have free energies ΔE_n with

$$\Delta E_0 > \Delta E_1 > \Delta E_2 > \cdots$$

BKT scaling

We can derive

$$\Delta_{\rm IR}(4-\Delta_{\rm IR}) = -m_{\rm IR}^2\ell_{\rm IR}^2 = G(\lambda_*, x) \ ,$$

where

$$G(\lambda, x) \equiv \frac{24a(\lambda)}{h(\lambda)(V_g(\lambda) - xV_{f0}(\lambda))} \ .$$

and by matching behaviors

$$\sigma \sim \frac{1}{r_{\rm UV}^3} \exp\left(-\frac{2K}{\sqrt{\lambda_* - \lambda_c}}\right) \sim \frac{1}{r_{\rm UV}^3} \exp\left(-\frac{2\hat{K}}{\sqrt{x_c - x}}\right) \ .$$

x_c and λ_c are defined by $G(\lambda_*(x_c), x_c) = 4$ and $G(\lambda_c, x) = 4$, respectively, so that $\lambda_* = \lambda_c$ at $x = x_c$. we obtain

$$K = \frac{\pi}{\sqrt{\frac{\partial}{\partial\lambda}G(\lambda_c, x)}} \ ; \qquad \hat{K} = \frac{\pi}{\sqrt{-\frac{d}{dx}G(\lambda_*(x), x)\Big|_{x=x_c}}} \ .$$

.

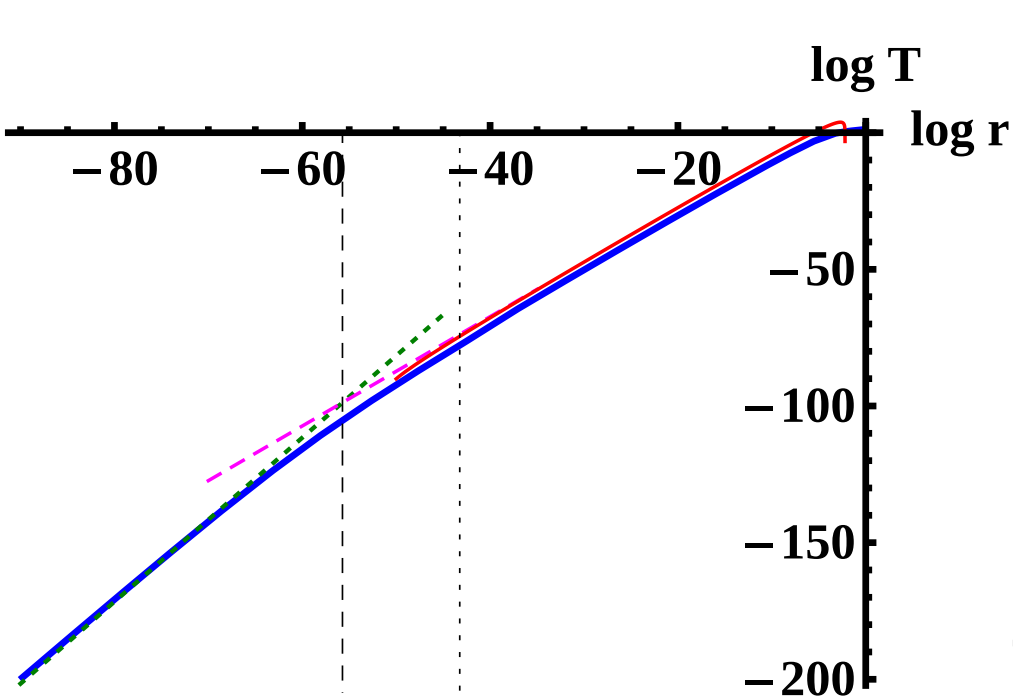

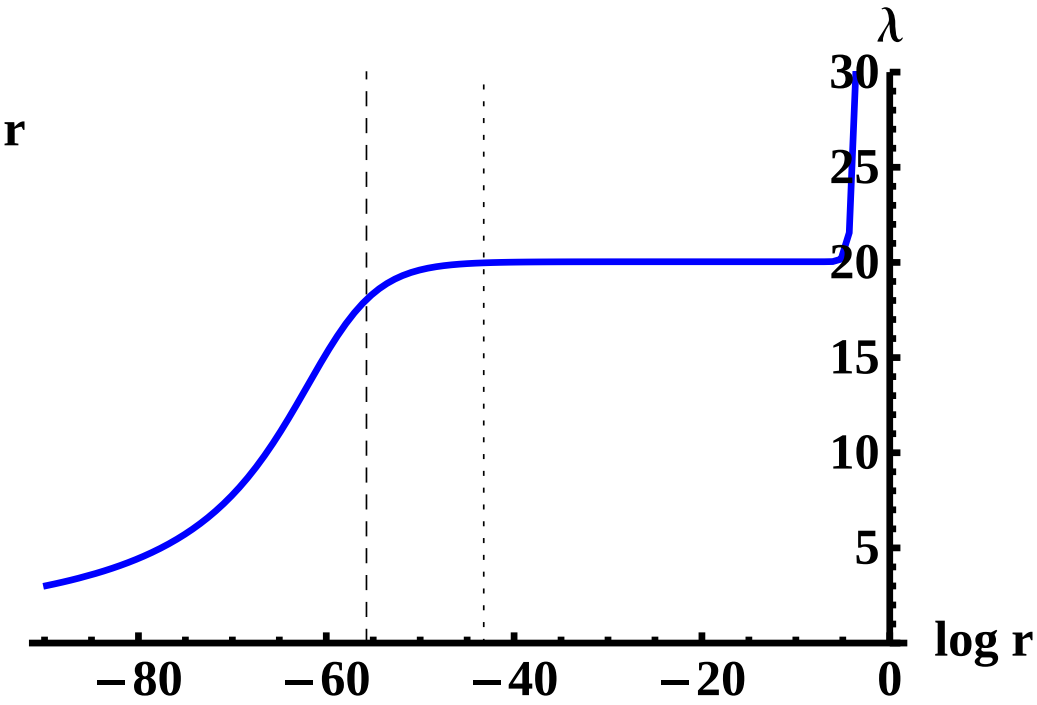

The tachyon $\log T$ (left) and the coupling λ (right) as functions of $\log r$ for an extreme walking background with $x = 3.992$. The thin lines on the left hand plot are the approximations used to derive the BKT scaling.

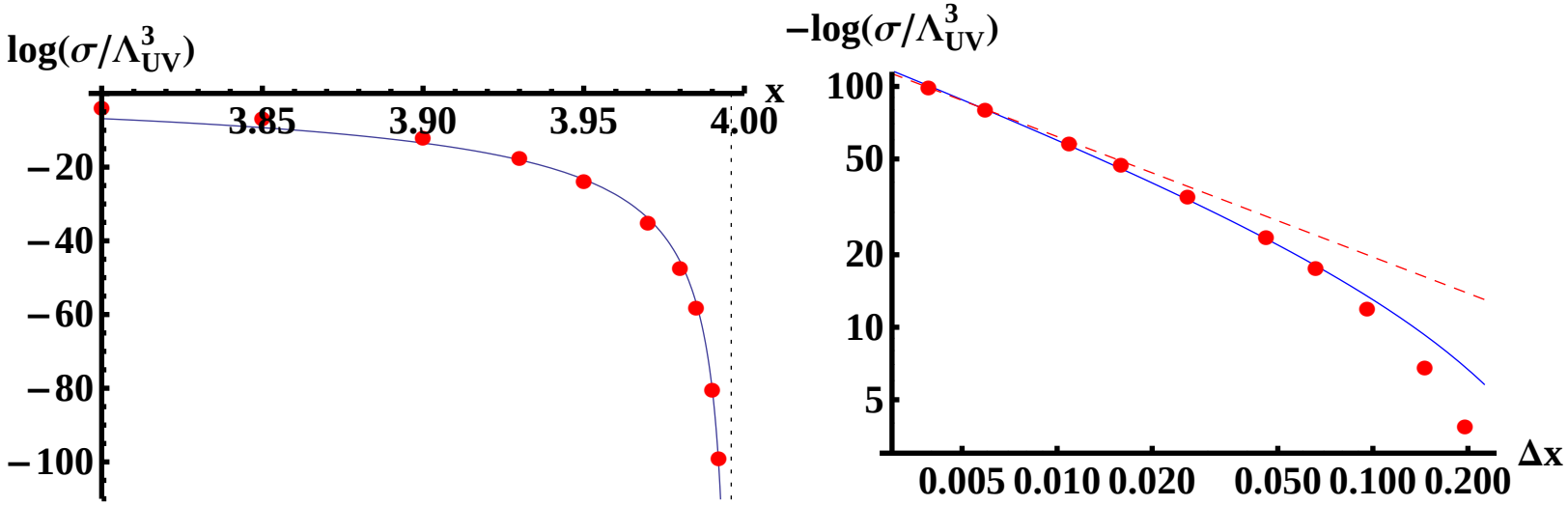

Left: $\log(\sigma/\Lambda^3)$ as a function of x (dots), compared to a BKT scaling fit (solid line). The vertical dotted line lies at $x = x_c$. Right: the same curve on log-log scale, using $\Delta x = x_c - x$.

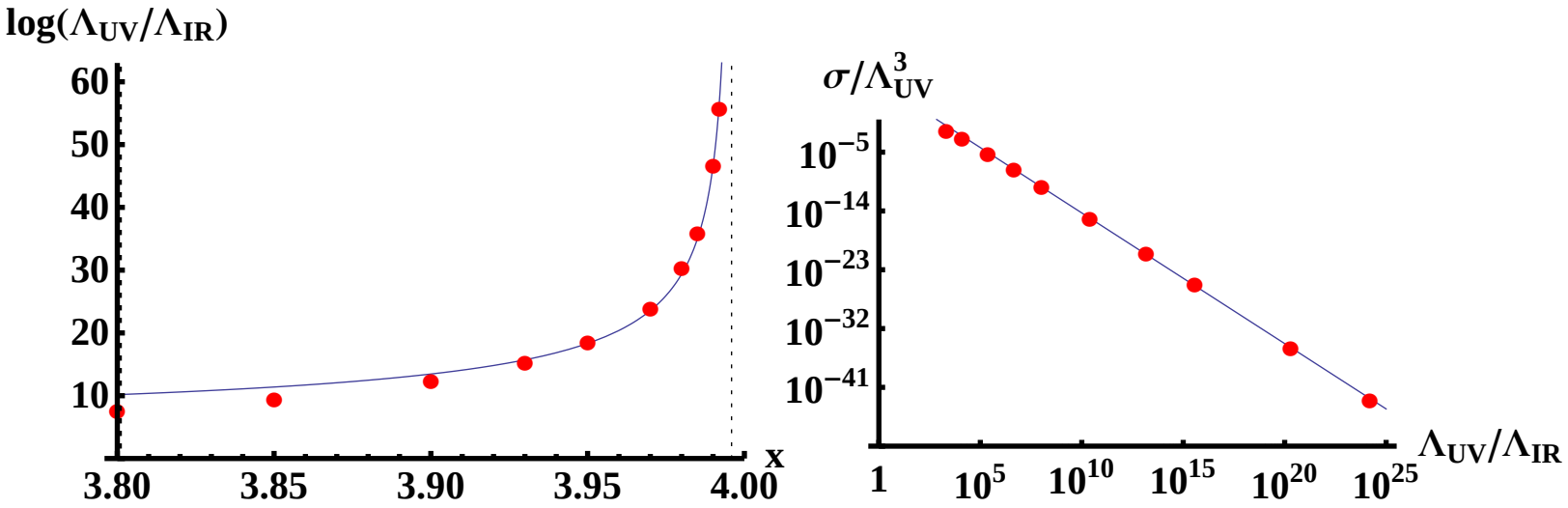

Left: $\log(\Lambda_{UV}/\Lambda_{IR})$ as a function of x (dots), compared to a BKT scaling fit (solid line). Right: σ/Λ^3 plotted against $\Lambda_{UV}/\Lambda_{IR}$ on log-log scale.

Comparison to N=1 sQCD

The case of $\mathcal{N} = 1$ $SU(N_c)$ superQCD with N_f quark multiplets is known and provides an interesting (and more complex) example for the non-supersymmetric case. From Seiberg we have learned that:

- $x = 0$ the theory has confinement, a mass gap and N_c distinct vacua associated with a spontaneous breaking of the leftover R symmetry Z_{N_c}.

- At $0 < x < 1$, the theory has a runaway ground state.

- At $x = 1$, the theory has a quantum moduli space with no singularity. This reflects confinement with χSB.

- At $x = 1 + \frac{1}{N_c}$, the moduli space is classical (and singular). The theory confines, but there is no χSB.

- At $1 + \frac{2}{N_c} < x < \frac{3}{2}$ the theory is in the non-abelian magnetic IR-free phase, with the magnetic gauge group $SU(N_f - N_c)$ IR free.

• At $\frac{3}{2} < x < 3$, the theory flows to a CFT in the IR. Near $x = 3$ this is the Banks-Zaks region where the original theory has an IR fixed point at weak coupling. Moving to lower values, the coupling of the IR $SU(N_c)$ gauge theory grows. However near $x = \frac{3}{2}$ the dual magnetic $SU(N_f - N_c)$ is in its Banks-Zaks region, and provides a weakly coupled description the IR fixed point theory.

• At $x > 3$, the theory is IR free.

There are similarities and important differences with QCD:

• sQCD contains scalars and this gives rise to an extended potential and moduli space that is responsible for most of differences.

• The chiral symmetry works differently.

• There is a similarity with the magnetic gauge group. Here it is generated by the axial and vector mesons that are massless in the conformal window. However, unlike sQCD here they are always weakly coupled in the IR because of the large N_c limit.

Outlook

There are many directions that need to be explored:

- The meson spectra at $T = 0$. Singlet mesons will mix with appropriate glueballs. Is the σ-meson a dilaton?.

- Computation of the S parameter for technicolor applications.

- The finite-temperature phase diagram is being investigated.
It shows a rich and unexpected structure in the walking region.

- Study energy loss of quarks in QGP (with full backreaction).

- The parameter x resembles somewhat the doping parameter in high-Tc superconductivity. Mesons should be thought of as Cooper pairs of axial charge.

- Study the phase diagram at finite density.

- "Model building": Construction of realistic technicolor models.

.

Thank you

Numerical solutions: $T = 0$

$T \equiv 0$ backgrounds (color codes λ, A)

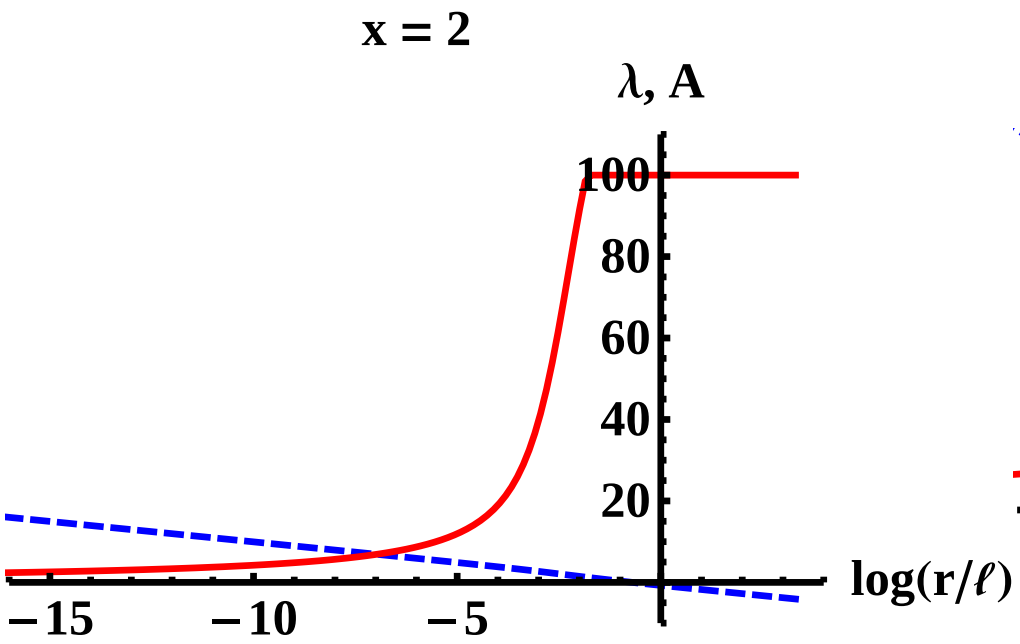

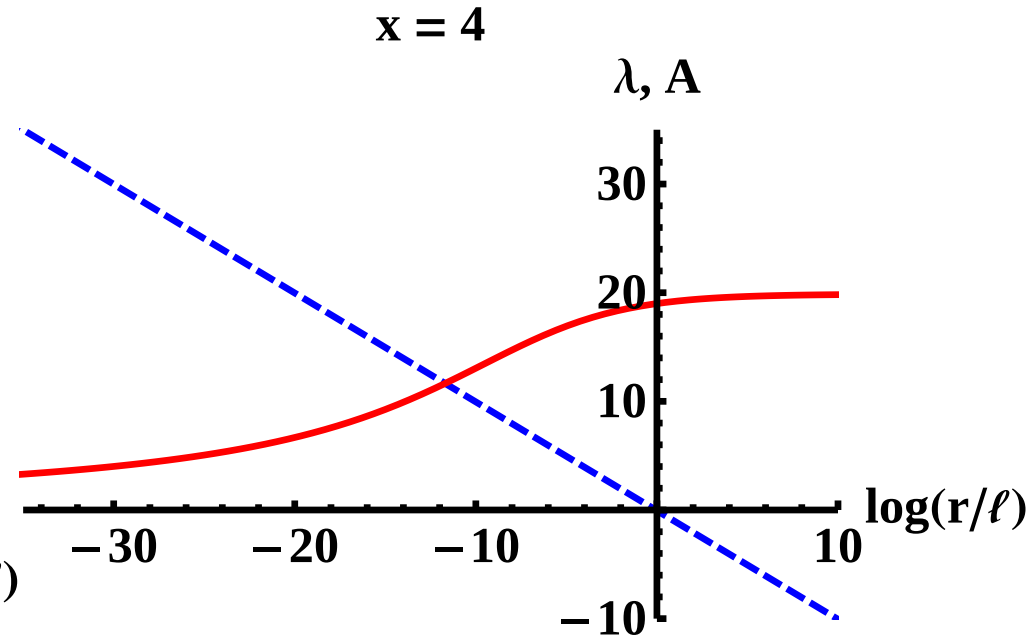

Numerical solutions: Massless with $x < x_c$

Massless backgrounds with $x < x_c \simeq 3.9959$ (λ, A, T)

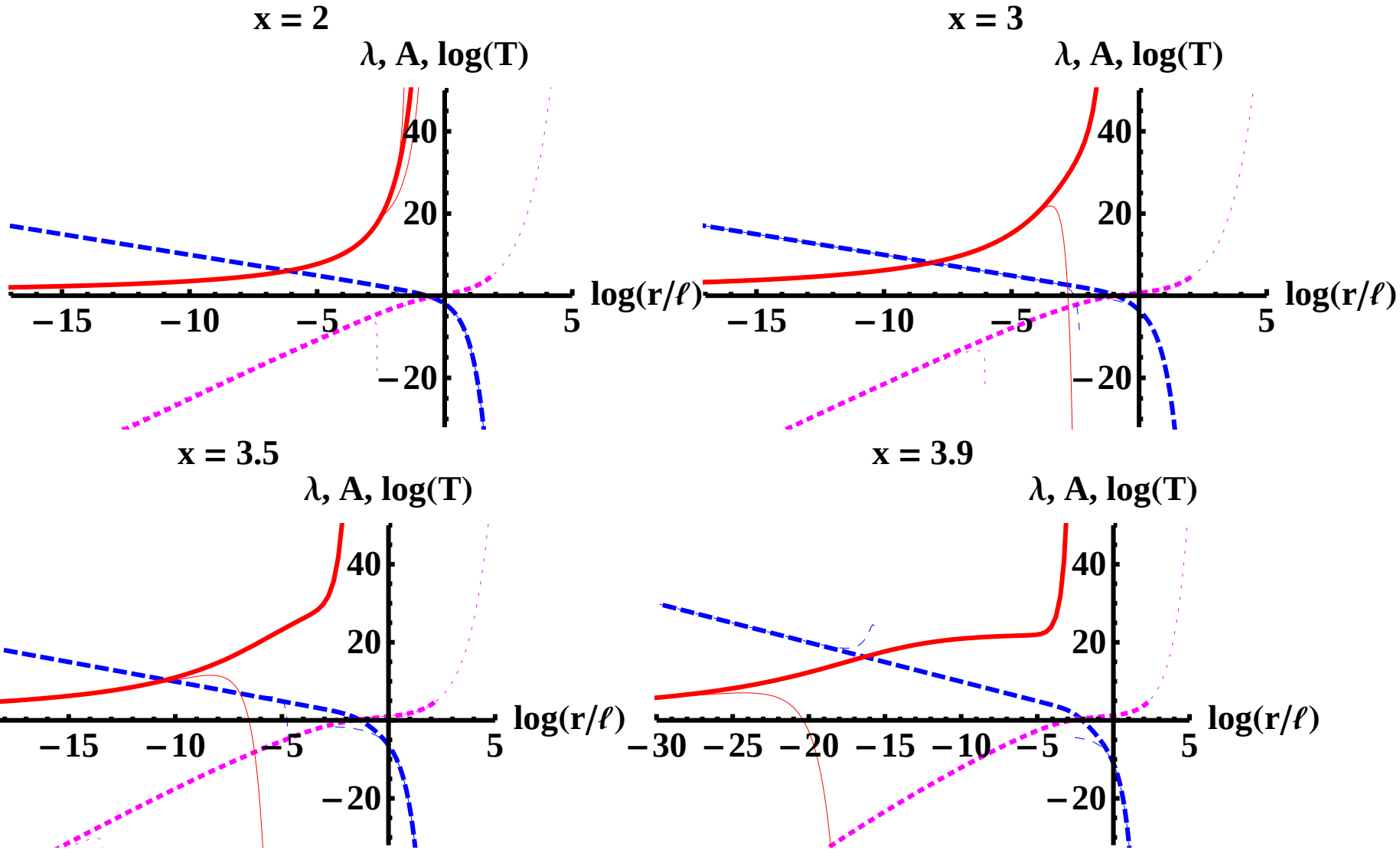

Massless backgrounds: beta functions $\beta = \frac{d\lambda}{dA}$, ($x_c \simeq 3.9959$)

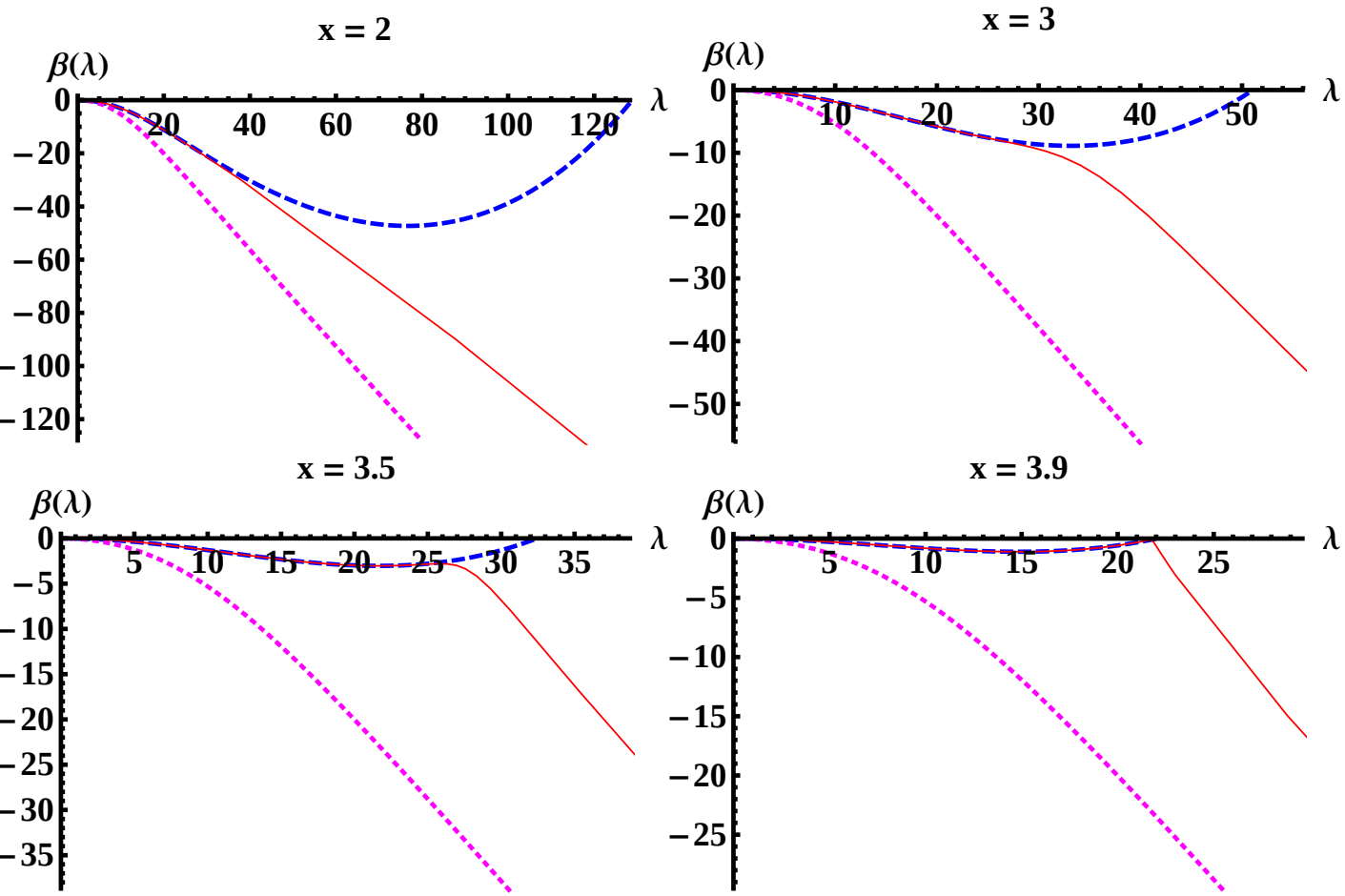

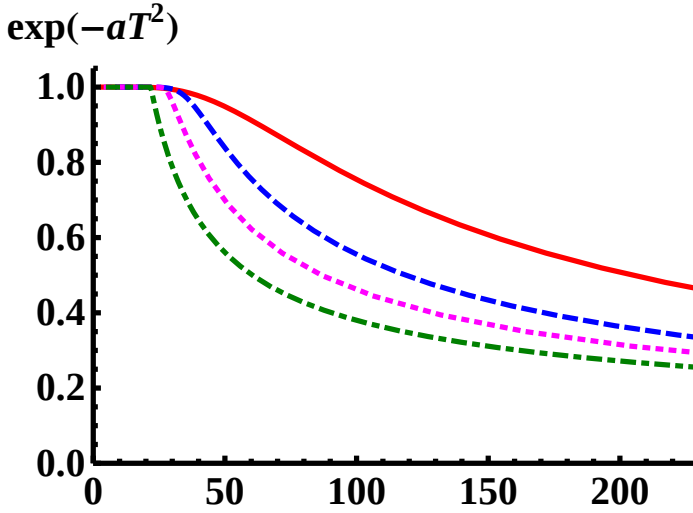

$x = 2, 3, 3.5, 3.9$

.

Massless backgrounds: gamma functions $\frac{\gamma}{T} = \frac{d \log T}{dA}$

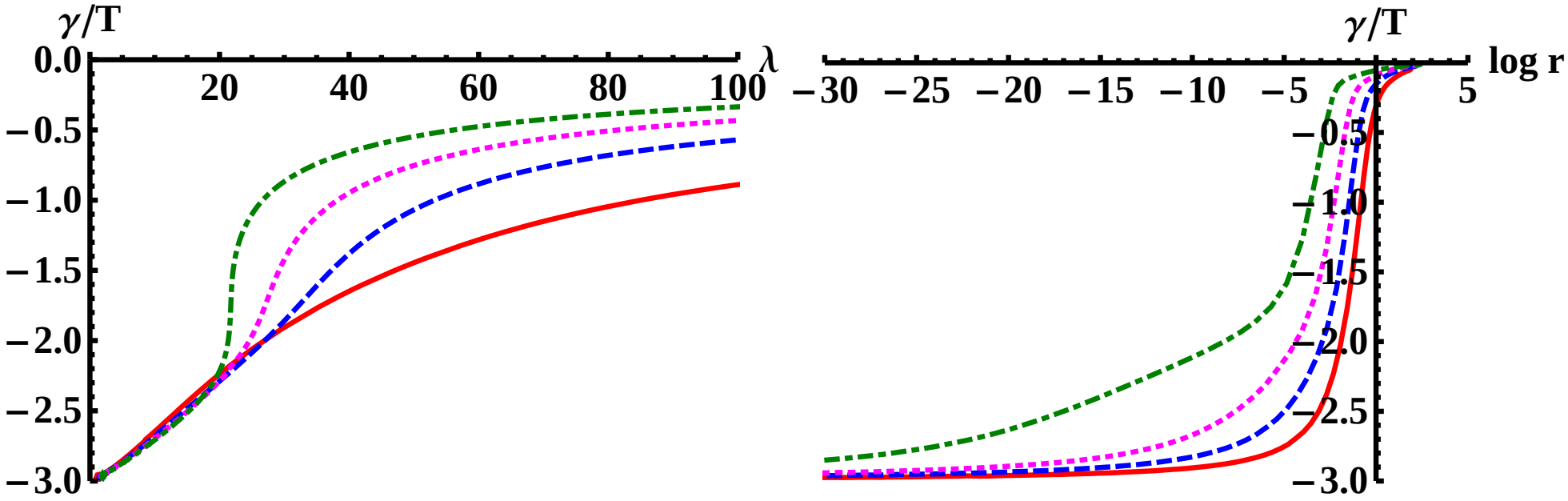

$x = 2, 3, 3.5, 3.9$

Detailed plan of the presentation

- Title page 0 minutes
- Bibliography 1 minutes
- Introduction 5 minutes
- The holographic models:glue 8 minutes
- YM entropy 9 minutes
- YM trace 10 minutes
- The speed of sound 11 minutes
- The holographic models:flavor 15 minutes
- The Veneziano Limit 17 minutes
- The Banks-Zaks region 19 minutes
- Fusion 21 minutes
- The effective potential 25 minutes
- Condensate dimension at the IR fixed point 27 minutes
- Below the BF bound 30 minutes
- Matching to QCD : UV 31 minutes
- Matching to QCD : IR 36 minutes

- Varying the model 38 minutes
- Comparison to previous guesses 39 minutes
- Holographic β-functions 42 minutes
- Parameters 43 minutes
- UV mass vs T_0 and r_1 49 minutes
- The free energy 51 minutes
- BKT scaling 56 minutes
- Comparison to N=1 sQCD 59 minutes
- Outlook 61 minutes

- Numerical solutions :$T = 0$ 63 minutes
- Numerical solutions: Massless with $x < x_c$ 68 minutes